Journal of Thermal Biology 81 (2019) 185–193

Contents lists available at ScienceDirect

Journal of Thermal Biology

journal homepage: www.elsevier.com/locate/jtherbio

Bats are not squirrels: Revisiting the cost of cooling in hibernating mammals

Catherine G. Haase[a,*], Nathan W. Fuller[b], C. Reed Hranac[c], David T.S. Hayman[c], Sarah H. Olson[d], Raina K. Plowright[a], Liam P. McGuire[b]

[a] *Department of Microbiology and Immunology, Montana State University, 109 Lewis Hall, PO Box 173520, Bozeman, MT 59717, USA*
[b] *Department of Biological Sciences, Texas Tech University, 2901 Main St., Lubbock, TX 79409, USA*
[c] *Molecular Epidemiology and Public Health Laboratory, Hopkirk Research Institute, Massey University, Private Bag, 11 222, Palmerston North 4442, New Zealand*
[d] *Wildlife Conservation Society, 2300 Southern Boulevard, Bronx, NY 10460, USA*

ARTICLE INFO

Keywords:
Bats
Cooling
Energetic model
Hibernation
Torpor
Winter survival

ABSTRACT

Many species use stored energy to hibernate through periods of resource limitation. Hibernation, a physiological state characterized by depressed metabolism and body temperature, is critical to winter survival and reproduction, and therefore has been extensively quantified and modeled. Hibernation consists of alternating phases of extended periods of torpor (low body temperature, low metabolic rate), and energetically costly periodic arousals to normal body temperature. Arousals consist of multiple phases: warming, euthermia, and cooling. Warming and euthermic costs are regularly included in energetic models, but although cooling to torpid body temperature is an important phase of the torpor-arousal cycle, it is often overlooked in energetic models. When included, cooling cost is assumed to be 67% of warming cost, an assumption originally derived from a single study that measured cooling cost in ground squirrels. Since this study, the same proportional value has been assumed across a variety of hibernating species. However, no additional values have been derived. We derived a model of cooling cost from first principles and validated the model with empirical energetic measurements. We compared the assumed 67% proportional cooling cost with our model-predicted cooling cost for 53 hibernating mammals. Our results indicate that using 67% of warming cost only adequately represents cooling cost in ground squirrel-sized mammals. In smaller species, this value overestimates cooling cost and in larger species, the value underestimates cooling cost. Our model allows for the generalization of energetic costs for multiple species using species-specific physiological and morphometric parameters, and for predictions over variable environmental conditions.

1. Introduction

Heterothermy is a thermoregulatory strategy employed by many mammals whereby body temperature (T_b) and metabolic rate are reduced in response to climatic conditions or reduced nutritional availability (Geiser, 1988; Lyman, 2013; Speakman and Thomas, 2003). Hibernation is an extreme form of extended heterothermy, which consists of cycles of torpor, or periods of low metabolic rate and T_b, and arousals, or periods of euthermic T_b (Geiser, 1988; Thomas et al., 1990). Each arousal consists of three phases: (1) warming from torpid T_b to euthermic T_b, (2) maintaining euthermic T_b, (3) and cooling from euthermic T_b back to torpid T_b. The energetics of hibernation are critical to winter survival, and hence this component of life history has been extensively quantified and modeled across many species (Hayman et al., 2016; Humphries et al., 2002; Thomas et al., 1990).

Although only a small fraction of hibernation is spent in euthermia, it accounts for up to 75–90% of winter energy budgets (Thomas et al., 1990). Because of the high energetic cost of arousal, most research has focused on quantifying these costs and how arousal frequency relates to energy budgets and survival (Geiser, 1988; Thomas et al., 1990; Wang, 1978). The energetic cost of warming has been calculated by a variety of models (Table 1), and all of these models focus on the temperature difference between euthermic and torpid T_b. This difference in T_b is scaled by the specific heat of animal tissue, which describes the energy required to warm 1 g of tissue by 1 °C (Wang, 1978). Beyond the cost to warming animal tissue, it is also important to consider the cost of maintaining metabolism during the time it takes to warm (typically against an environmental gradient of cool ambient temperature [T_a] relative to T_b). McKechnie and Wolf (2004) added this additional cost with the calculation of metabolism over the period of warming. Cryan and Wolf (2003) then incorporated the effect of thermal conductance on warming, accounting for heat lost to the environment. Both of these

---

[*] Corresponding author.
E-mail address: catherine.haase@montana.edu (C.G. Haase).

https://doi.org/10.1016/j.jtherbio.2019.01.013
Received 16 August 2018; Received in revised form 18 December 2018; Accepted 21 January 2019

Table 1
Summary of previous studies that calculated energy expenditure during torpor or arousals, including the various methods by which warming and cooling costs have been considered. Warming models consider the effects of body mass (M_b), specific heat capacity of tissues (S), euthermic (T_{eu}) and torpid (T_b) body temperatures, and resting (RMR) and torpid (TMR) metabolic rates.

Species	Warming model	Cooling use	Reference
Various bats	$M_b(T_{eu} - T_{tor})S$	None	(Prothero and Jürgens, 1986)
Myotis lucifugus	$(T_{eu} - T_{tor})S$	67.2% of warming	(Thomas et al., 1990)
Myotis lucifugus	$(T_{eu} - T_{tor})S$	None	(Humphries et al., 2002)
Lasiurus cinereus	$M_b(T_{eu} - T_{tor})S + \int_{t_1}^{t_2} C(T_{eu} - T_a)$	None	(Cryan and Wolf, 2003)
Lasiurus cinereus	$[M_b(T_{eu} - T_{tor})S] + D^*_{warm}\left(TMR + \frac{RMR - TMR}{2}\right)$	None	(Willis et al., 2006)
Myotis lucifugus	$(T_{eu} - T_{tor})S$	65% of warming	(Frederico, 2007)
Myotis lucifugus	$(T_{eu} - T_{tor})S$	67% of warming	(Boyles and Brack, 2009)
Myotis lucifugus	$(T_{eu} - T_{tor})S$	67% of warming	(Boyles and McKechnie, 2010)
Various bats	$(T_{eu} - T_{tor})S$	67% of warming	(Boyles and Willis, 2010)
Myotis lucifugus	$(T_{eu} - T_{tor})S$	67% of warming	(Jonasson and Willis, 2012)**
Myotis lucifugus	$(T_{eu} - T_{tor})S$	67% of warming	(Ehlman et al., 2013)
Myotis lucifugus	None	None	(Burles et al., 2014)
Lasionycteris noctivagans	$M_b(T_{eu} - T_{tor})S + \int_{t_1}^{t_2} C(T_{eu} - T_a)$	67.2% of warming	(McGuire et al., 2014)
Various bats	$(T_{eu} - T_{tor})S$	None	(Hayman et al., 2016)
Myotis lucifugus	$[M_b(T_{eu} - T_{tor})S] + D^*_{warm}\left(TMR + \frac{RMR - TMR}{2}\right)$	67.2% of warming	(Wilcox and Willis, 2016)
Myotis lucifugus	$(T_{eu} - T_{tor})S$	67.2% of warming	(Czenze et al., 2017)

*D_{warm} is defined as the time required to warming tissues, a function of the rate of warming and gradient between euthermic and torpid body temperatures.
**Jonasson and Willis (2012) also used models published by Thomas et al. (1990) and Humphries et al. (2002) listed in the table.

models also incorporated the effects of warming rate, which is found to scale with body mass in both mammals and birds (Geiser and Baudinette, 1990; McKechnie and Wolf, 2004).

Cooling is also an important phase of the torpor-arousal cycle; however, this phase has been overlooked in modeling hibernation energetics (Henshaw, 1968; Kleiber, 1972). Most models of hibernation energetics have either used an assumed cost of cooling calculated from the cost of warming or excluded the cooling phase entirely (Table 1). Cooling is typically considered a passive process (but see discussions of metabolic suppression: Drew et al., 2007; Geiser, 2004; Heldmaier and Ruf, 1992; Snapp and Heller, 1981; Staples, 2014) and therefore requires less energy than warming (Geiser, 2004, 1988). However, the cooling phase still requires energy for metabolism over the period of time it takes to cool (Thomas et al., 1990; Wang, 1978), which can vary among taxa.

The energetic cost of cooling was first measured by Wang (1978) in Richardson's ground squirrels (*Urocitellus richardsonii*, formerly *Spermophilus richardsonii*) across winter hibernation at a range of T_a. Thomas et al. (1990) used Wang's measurements to calculate cooling cost as a proportion of warming cost, regardless of temperature, and found cooling costs were equivalent to 65–67% of the cost of warming. As the Thomas et al. (1990) energetic model has been frequently applied and revised, many subsequent hibernation energetic models have assumed the same proportional cost of cooling (Table 1). It is unclear whether this proportion is broadly representative across taxa.

We suspect that assuming proportional cooling costs could be problematic in other taxa for three reasons: differences in body size, differences in thermal conductance, and the influence of T_a on cooling rate. Estimates of cooling cost by the 67% proportion may overestimate cost in small-bodied species or underestimate cost for larger species due to the relationship between body mass and surface area (Berman, 2003; Gouma et al., 2012; Meeh, 1879). The higher surface area to volume ratio in smaller species lead to a greater rate of heat loss, and thus, for species smaller than Richardson's ground squirrels (the basis for the proportional cost estimate), there is a potential for a lower cooling cost than that predicted by 67% of warming. Additionally, thermal conductance has been observed to scale with body mass (Aschoff, 1981; Kleiber, 1972), and thus large-bodied species not only have greater body mass to cool, but are more resistant to heat loss. Thermal conductance can also vary within similar-sized species that reside in variable environments (Aschoff, 1981; Anon, 1987). Thus, it is possible that cooling rate may be more affected by T_a than warming rate due

Table 2
Measured and modeled costs (ml O_2 g^{-1}) of cooling into torpor from euthermia. Measured costs are reported from the referenced papers and modeled costs are from Eq. (2).

Species	T_a (°C)	Measured Costs	Modeled Costs	Data Reference
Erinaceus europaeus	5	4.73	4.65	Webb and Ellison (1998)
Glis glis	4	2.65	2.86	Wilz and Heldmaier (2000)
Marmota flaviventris	6	9.25	8.53	Armitage et al. (2003)
Marmota marmota	7	3.76	3.86	Heldmaier et al. (2004)
Urocitellus richardsonii	13–15	4.22[a]	4.50[b]	Wang (1978)
Urocitellus richardsonii	8–10	3.16[a]	3.85[b]	Wang (1978)
Urocitellus richardsonii	2–6	4.09[a]	3.98[b]	Wang (1978)
Zapus princeps	5	5.09	5.17	Cranford (1983)

[a] mean over all individuals.
[b] mean over all temperatures.

differences in physical and physiological processes in each phase (Nicol and Andersen, 2007), and therefore cooling cost may have higher variation with T_a compared to warming cost.

Many applications of the 67% cooling cost assumption have focused on bats (Table 1), which may have very different physiologies and cooling properties compared to ground squirrels (Bakken, 1976a; Strunk, 1971). Appropriately modeling hibernation energetics is important for understanding the impacts of white-nose syndrome (WNS) (Hayman et al., 2016), a disease of hibernating bats caused by an invasive fungal pathogen (Blehert et al., 2009; Lorch et al., 2013; Warnecke et al., 2012). WNS causes an increase in arousal frequency (Reeder et al., 2012; Warnecke et al., 2012), leading to premature depletion of fat stores and death (Hayman et al., 2016). Many studies have focused on the energetics associated with hibernation and WNS (Hayman et al., 2016; Mayberry et al., 2018; McGuire et al., 2017; Warnecke et al., 2013; Willis, 2015; Willis et al., 2011), and therefore energetic models represent an important tool for understanding the costs and consequences of the disease. This approach is especially timely as evidence suggests species differ in their susceptibility and response to WNS, due in part to interspecific variation in morphology and physiology, and microclimate selection during hibernation (Langwig et al., 2016; Langwig et al., 2012; Willis, 2015).

We investigated the energetic cost of cooling to determine if previous estimates are applicable across taxa. We developed a mathematical model to calculate the cost of cooling given the change in metabolic rate between euthermia and torpor and the rate at which an animal cools. Cooling rate was calculated using Newton's law of cooling (Bakken, 1976a; Newton, 1701; Prothero and Jürgens, 1986), which considers body mass, surface area, and thermal conductance in addition to the difference between euthermic T_b and T_a. We also determined if mass-specific cooling cost could be predicted by cooling rate. We then applied our model to a variety of species to test whether modeled cooling cost matched the oft cited 67% of warming cost and determined if any variation in the relationship is better described by differences in body size. Finally, given the scaling relationship found between body mass and warming rate, we determined if cooling rate could be predicted by body mass.

2. Materials and methods

2.1. Energetic costs of cooling

We modeled the energetic cost of cooling (E_{cool}) as a function of the difference between euthermic and torpid T_b, the decrease in metabolic rate over that temperature range, and the cooling rate. We assumed that cooling occurred passively; that is, the reduction in metabolic rate is due to an effect of temperature, rather than physiological inhibition (but see Geiser, 2016, 2004).

We calculated the total cost of cooling as the energy required for metabolism during steady-state torpor, plus the additional costs to maintain metabolism above torpid T_b as the body cools from euthermic T_b (Prothero and Jürgens, 1986; Strunk, 1971). We calculated this change using Q_{10}, or the change in metabolic rate over a 10 °C change in temperature, with a scaling equation with body mass (M_b; g)(Geiser, 1988):

$$Q_{10} = 3.82 - 0.507\log_{10}M_b \tag{1}$$

The cost of cooling was therefore calculated as the sum of this reduction in euthermic metabolic rate in response to the difference between torpid and euthermic T_b, and the metabolic rate of steady-state torpor:

$$E_{cool} = D_{cool}\left[TMR_{min} + \left(RMR \bullet Q_{10}^{\frac{T_{tor}-T_{eu}}{10}}\right)\right] \tag{2}$$

where TMR_{min} is the mass-specific minimum torpid metabolic rate (ml O_2 g^{-1} h^{-1}), RMR is the mass-specific resting metabolic rate at T_a (ml O_2 g^{-1} h^{-1}), T_{tor} and T_{eu} are torpid and euthermic T_b (°C), respectively, and D_{cool} is the duration of the cooling phase (h). We estimated RMR by increasing allometrically predicted BMR (Schmidt-Nielsen, 1984; Speakman and Thomas, 2003) in response to T_a and scaled by euthermic thermal conductance (C):

$$RMR = BMR + C(T_{eu} - T_a) \tag{3}$$

The duration of the cooling phase (D_{cool}) was determined by the cooling rate (CR) and the temperature difference between T_b:

$$D_{cool} = \frac{\log(T_{eu} - T_{tor})}{CR} \tag{4}$$

We assumed that cooling followed an exponential decay (Newton, 1701). Therefore we modeled the rate of cooling as a derivation from Newton's Law of Cooling (Henshaw, 1968; Kleiber, 1972; Newton, 1701; Strunk, 1971), which assumes the rate of heat loss from a body is directly proportional to body size, conductance, and temperature difference between the body and the surrounding environment (Bakken, 1976a; Prothero and Jürgens, 1986). We calculated the cooling rate as:

$$CR = \frac{C \bullet M_b^{0.67} \bullet \log(T_{eu} - T_a)}{S \bullet M_b} \tag{5}$$

where C is the thermal conductance during euthermia (ml O_2 g^{-1} °C^{-1} h^{-1}), $M_b^{0.67}$ represents the surface area of the animal as defined by body mass, $T_{eu} - T_a$ is the difference between euthermic T_b and T_a (°C), and S is the specific heat of animal tissue (0.1728 ml O_2 g^{-1} °C^{-1}; Hart, 1951). By taking the log of the temperature difference in both Eqs. 4 and 5, we account for the exponential change in the rate of cooling as T_b is reduced to torpid body temperature. Rather than estimating an instantaneous cooling rate, this equation allowed for the consideration of body size and insulation of the animal (i.e. thermal conductance), as well as environmental influences (e.g., rapid cooling in cold environments).

Table 3

Parameters used to apply cooling model across mammalian species: cooling rate (CR; °C h^{-1}), warming rate (W*R*; °C h^{-1}), body mass (M_b; g), thermal conductance (C; ml O_2 g^{-1} $°C^{-1}$), euthermic (T_{eu}; °C) and torpid (T_{tor}; °C) body temperature, air temperature (T_a; °C), and Q_{10} rates.

Species, by order	CR	W*R*	M_b	C	T_{eu}	T_{tor}	T_a	Q_{10}	Reference [Conductance Reference]
Chiroptera									
Chalinolobus gouldii	1.29	84.0	12	0.34	36	6	5	3.27	Hosken and Withers (1997)
Corynorhinus townsendii	0.80	91.2[a]	10	0.20	37	9	8	3.32	CGH et al. (Unpublished data) Speakman and Thomas (2003)
Eptesicus fuscus	0.61	90.0[b]	18	0.20	37	16	15	3.19	Halsall et al. (2012) and Willis (2015)
Lasionycteris noctivagans	0.59	162.0[b]	11	0.15	35	6	5	3.30	Dunbar (2007)
Lasiurus borealis	0.46	106.8[b]	13	0.13	35	6	5	3.26	Dunbar and Tomasi (2006)
Lasiurus cinereus	0.53	128.4[b]	25	0.18	35	6	5	3.11	Cryan and Wolf (2003)
Myotis californicus	1.26	77.4[a]	5	0.26	35	11	10	3.47	CGH et al. (Unpublished data) Speakman and Thomas (2003)
Myotis lucifugus	1.11	64.0[a]	9	0.26	37	5	4	3.33	Czenze and Willis (2015) and Hayman et al. (2016)
Myotis myotis	0.51	24.2[a]	25	0.20	35	17	16	3.11	Wojciechowski et al. (2007)
Myotis nattereri	0.77	63.0[a]	8	0.18	35	10	8	3.36	Hope and Jones (2012) and Speakman and Thomas (2003)
Myotis velifer	0.70	50.0	14	0.20	37	9	8	3.23	CGH et al. (Unpublished data) Hirshfeld and O'Farrell (1976)
Myotis yumanensis	0.72	27.6	6	0.15	37	9	8	3.44	Licht and Leitner (1967) and O'Farrell and Studier (1970)
Nyctalus noctula	0.21	94.8[a]	27	0.07	37	5	5	3.09	Kayser (1964)
Nyctophilus geoffroyi	1.57	80.4[b]	8	0.36	36	6	6	3.37	Geiser and Brigham (2000) and Herreid and Kessel (1967)
Pipistrellus pipistrellus	1.10	57.0[a]	6	0.23	37	6	5	3.43	Kayser (1964)
Tadarida brasiliensis	0.90	43.8[a]	12	0.25	36	11	10	3.27	Herreid and Schmidt-Nielsen (1966)
Tadarida teniotis	0.45	46.8[a]	30	0.18	35	22	15	3.07	Marom et al. (2006)
Dasyuromorphia									
Dasyuroides byrnei	0.21	33.0[a]	120	0.13	34	11	10	2.77	Geiser and Baudinette (1987)
Planigale gilesi	1.19	57.0	8	0.33	33	10	15	3.36	Geiser and Baudinette (1988) and Stone and Purvis (1992)
Sminthopsis macroura	0.50	8.0[a]	28	0.22	34	21	19	3.09	Song et al. (1995)
Diprotodontia									
Burramys parvus	0.32	26.4[a]	54	0.14	36	3	2	2.94	Fleming (1985) and Herreid and Kessel (1967)
Cercartetus concinnus	0.70	47.4[a]	17	0.21	34	6	5	3.20	Geiser (1987)
Cercartetus lepidus	0.78	54.0[a]	12	0.21	34	6	5	3.27	Geiser (1987)
Cercartetus nanus	0.22	24.0[a]	70	0.11	35	6	5	2.88	Song et al. (1997)
Eulipotyphla									
Crocidura leucodon	0.61	54.0[a]	12	0.20	36	24	20	3.27	Nagel (1977)
Crocidura russula	0.69	54.0[a]	14	0.20	36	19	10	3.24	Nagel (1977)
Crocidura suaveolens	1.56	54.0[a]	8	0.37	36	20	10	3.38	Nagel (1977)
Erinaceus europaeus	0.19	10.2	505	0.18	34	11	10	2.45	Webb and Ellison (1998)
Rodentia									
Baiomys taylori	1.44	20.4	6	0.39	36	22	20	3.41	Hudson (1965)
Callospermophilus lateralis	0.18	20.0	137	0.12	35	16	15	2.74	Larkin and Heller (1996) and Snapp and Heller (1981)
Chaetodipus californicus	0.70	54.6	22	0.23	34	11	5	3.14	Tucker (1965)
Chaetodipus hispidus	0.47	21.0	40	0.21	38	18	17	3.01	Wang and Hudson (1970)
Cricetus cricetus	0.15	30.0[a]	370	0.13	35	10	8	2.52	Waßmer and Wollnik (1997) and Kayser (1964)
Eliomys quercinus	0.34	54.0[a]	80	0.17	33	6	5	2.86	Pajunen (1970) and Kayser (1964)
Glis glis	0.20	51.0[a]	100	0.11	36	8	8	2.81	Wilz and Heldmaier (2000) and Kayser (1961)
Ictidomys mexicanus	0.18	21.0[a]	190	0.14	36	15	17	2.66	Neumann and Cade (1965) and Snyder and Nestler (1990)
Ictidomys tridecemlineatus	0.16	27.0[a]	190	0.11	35	7	6	2.66	Pohl and Hart (1965) and Aschoff (1981)
Marmota broweri	0.03	2.9	2400	0.04	30	10	2	2.11	Lee et al. (2016)
Marmota flaviventris	0.02	2.3	3405	0.04	36	9	8	2.03	Arnold (1988) and Florant and Heller (1977)
Marmota marmot	0.02	5.0[a]	3870	0.04	34	10	7	2.00	Ortmann and Heldmaier (2000) and Kayser (1964)
Mesocricetus auratus	0.35	25.8[a]	80	0.17	37	5	4	2.86	Lyman (1948)
Microdipodops pallidus	0.53	48.0[a]	15	0.15	39	9	8	3.22	Bartholomew and MacMillen (1961)
Muscardinus avellanarius	0.87	66.0[a]	15	0.26	36	11	10	3.22	Pretzlaff and Dausmann (2012)
Otospermophilus beecheyi	0.11	2.6	502	0.12	32	15	14	2.45	Strumwasser (1959) and Aschoff (1981)
Perognathus longimembris	1.18	24.0[a]	8	0.27	35	5	3	3.35	Bartholomew and Cade (1957)
Phodopus sungorus	0.32	8.7	31	0.13	32	18	12	3.07	Heldmaier et al. (2004)
Sicista betulina	1.53	72.0[a]	10	0.38	38	6	5	3.31	Johansen and Krog (1959)
Spermophilus citellus	0.15	24.0[a]	290	0.11	36	6	1	2.57	Hut et al. (2002) and Aschoff (1981)
Tamias amoenus	0.52	56.0[a]	50	0.21	38	3	1	2.96	Geiser and Kenagy (1988) and Kenagy and Vleck (1982)
Tamias striatus	0.25	60.0[a]	92	0.13	35	6	5	2.82	Neal (1976) and Wang and Hudson (1970)
Urocitellus parryii	0.14	7.0	406	0.11	35	0	− 2	2.50	Boyer and Barnes (1999) and Hock (1960)
Urocitellus richardsonii	0.19	9.4	400	0.17	37	10	10	2.50	Wang (1978) and Snyder and Nestler (1990)
Zapus princeps	0.72	60.0[a]	26	0.25	33	6	5	3.10	Cranford (1983)
Monotremata									
Tachyglossus aculeatus	0.01	4.3	4600	0.03	33	2	2	1.96	Grigg et al. (1992) and Nicol and Andersen (2007)

[a] Geiser and Baudinette (1990).

[b] Menzies et al. (2016).

2.2. Model validation

To validate the cooling equation, we compiled data from published papers that presented metabolic rate and skin temperature curves over time and compared the total energetic cost of torpor entry (i.e., cooling) with modeled cost (Table 2). For publications where data was only presented in figures, we used plot digitizing software (WebPlotDigitizer 4.1; https://apps.automeris.io/wpd) to extract metabolic rate and skin temperature over the period of cooling. We calculated the mean of euthermic and torpid skin temperatures and defined the onset of cooling when skin temperature dropped at least 2 °C below mean euthermic skin temperature and the end of cooling when skin temperature was within 0.5 °C of mean torpid skin temperature. We extracted metabolic rate for the cooling curve at one-hour intervals from the start and end of cooling and summed the values over the entire cooling period.

Using Eq. (2), we then modeled the energetic cost of cooling given morphometric, physiological, and environmental parameters reported in each publication. We obtained body mass, torpid and euthermic T_b, and thermal conductance (if available) for each species; if thermal conductance was not available, we calculated conductance using methodology described by McNab (1969) and Speakman and Thomas (2003). RMR was predicted using Eq. (3) and TMR was predicted using the Q_{10} decrease in BMR in response to torpid T_b (Geiser, 1988). One publication (Wang, 1978) reported cooling costs for multiple individuals over three ranges of T_a. Therefore, we calculated the mean cost for each temperature range over individuals (for the measured cost) and temperatures (for modeled cost). In instances where multiple data sources existed for the same species (as in the case of *Myotis lucifugus*), we chose the source that reported as many model parameters as possible.

We compared our modeled values to measured values using linear regression in R version 3.3.3 (R Development Core Team, 2009). We assumed that if our cooling model adequately represented measured cooling cost, the slope of the relationship would not be different than 1 (Glantz and Slinker, 2000). We did not run a sensitivity analysis of the model to changes in parameters, as a preliminary analysis showed that the model was sensitive to all parameters equally.

We examined the relationship between mass-specific cooling cost and both body size and thermal conductance to determine the effects of each variable on cooling. We also determined if a scaling relationship with body size and mass-specific cooling cost existed with cooling rate, similar to the relationships observed with warming rate (Geiser and Baudinette, 1990; McKechnie and Wolf, 2004).

2.3. Comparison between 67% proportion and cooling model

We compared the energetic cost of cooling for 53 species (Table 3) using both our cooling model (Eq. (2)) and the commonly-assumed 67% proportion of warming cost. We defined the energy required to warm from torpor to euthermia (E_{warm}) as a function of the cost to raise the temperature of animal tissue from torpid to euthermic T_b (McKechnie and Wolf, 2004), in addition to the metabolic costs required to balance heat lost to the environment over the period of warming (Cryan and Wolf, 2003). Thus, the cost of warming was calculated as:

$$E_{warm} = S\bullet(T_{eu} - T_{tor}) + D_{warm}[C(T_{eu} - T_a)] \tag{6}$$

where D_{warm} is the duration of time required to warm from torpid to euthermic T_b (h). Assuming warming occurs linearly (Cryan and Wolf, 2003; McKechnie and Wolf, 2004), we calculated D_{warm} as:

$$D_{warm} = \frac{T_{eu} - T_{tor}}{WR} \tag{7}$$

where WR is the warming rate for the species (°C h^{-1}). We obtained warming rates for each species from multiple sources (Geiser and Baudinette, 1990; Hirshfeld and O'Farrell, 1976; Menzies et al., 2016; Willis, 2008). All other model parameters were acquired as described above.

We compared both estimates of cooling, predicted from Eq. (2) and estimated as 67% of warming, using linear regression. If 67% of warming sufficiently described the cost of cooling, we assumed the slope of the relationship not to be different from 1 (Glantz and Slinker, 2000). We regressed the difference between the two estimates against body mass to examine differences in predicted cooling costs in the context of body size.

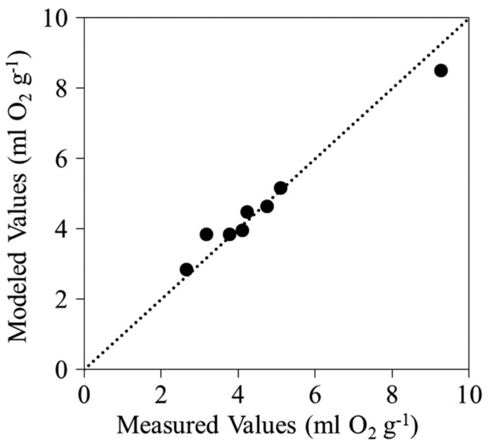

Fig. 1. Measured and modeled cooling cost (ml O_2 g^{-1}) of hibernating species used to validate a cooling cost model. Dashed line represents 1:1 line. Modeled cost was not different from measured cost (*slope* = 0.99 [0.939, 1.04], $F_{1,7}$ = 1220, p = < 0.001, r^2 = 0.99).

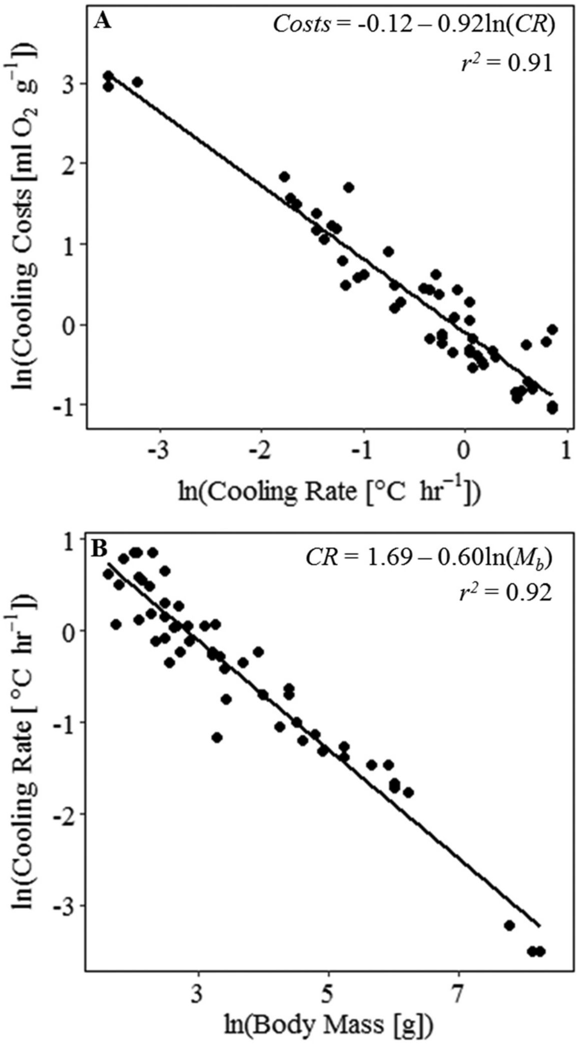

Fig. 2. Relationship between cooling rate (CR; °C h^{-1}) and A) body mass (g) and B) mass-specific cooling cost per arousal (ml O_2 g^{-1}) for 53 mammalian hibernators.

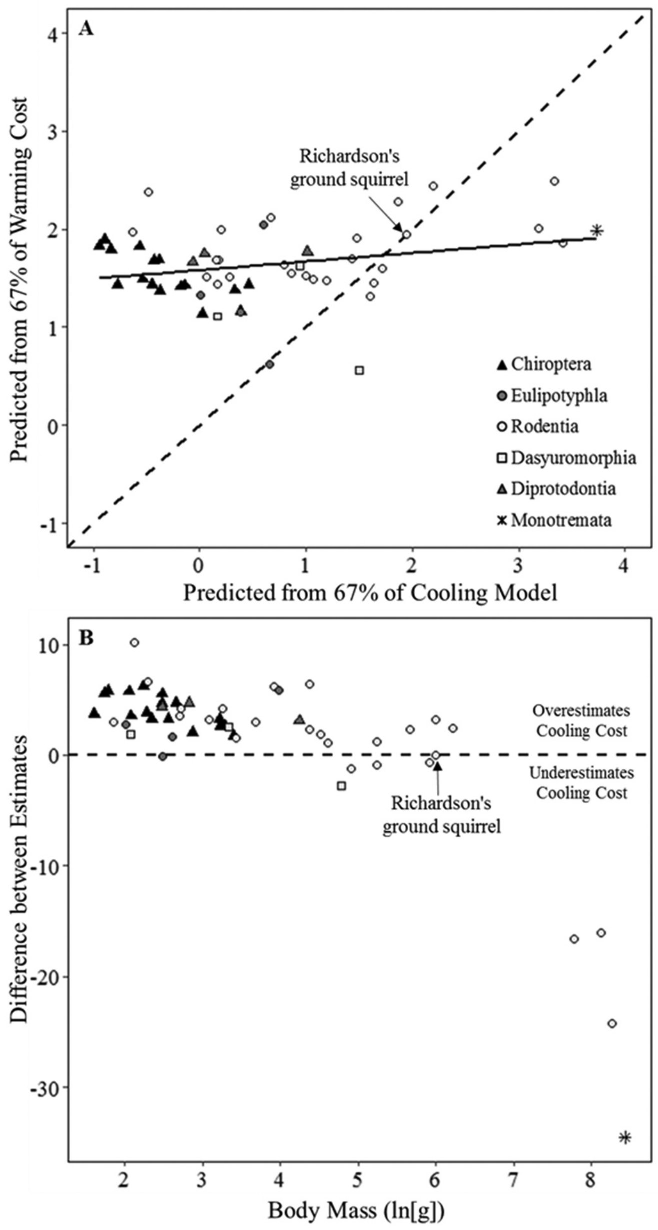

Fig. 3. A) Energetic cost of cooling (ln[ml O_2 g^{-1}]) for 53 mammalian species grouped by order and predicted from our cooling model and estimated from the commonly assumed 67% of warming costs. Dashed line represents one-to-one relationship between estimates and solid line is the fitted relationship. B) Relationship of the difference between cooling cost estimates (predicted from 67% of warming cost – cooling model; ml O_2 g^{-1}) and body mass (ln[g]). Dashed line represents 0 difference between estimates.

3. Results

Cooling cost from our model was not different from measured cost (*slope* = 0.99 [0.93, 1.04], $F_{1,7}$ = 1220, p = < 0.001, r^2 = 0.99; Table 2, Fig. 1). Mass-specific costs of cooling ranged from 0.36 ml O_2 g^{-1} in the Northern birch mouse (*Sicista betulina* [10 g]), one of the smallest species, to 41.9 ml O_2 g^{-1} in the short-beaked echidna (*Tachyglossus aculeatus* [4600 g]), the largest species in our dataset. Warming ranged from 2.8 ml O_2 g^{-1} in the bicolored shrew (*Crocidura leucodon* [12 g]) to 26.4 ml O_2 g^{-1} in the arctic ground squirrel (*Urocitellus parryii* [406 g]). Cooling was more energetically costly than warming in four species (*Marmota flaviventris, M. broweri, M. marmota,* and *T. aculeatus*), all of which had low thermal conductance values (< 0.05 ml O_2 g^{-1} °C^{-1} h^{-1}), large body sizes (> 2000 g), and thus slow cooling rates (< 0.5 °C h^{-1}).

Both body mass and thermal conductance were significant predictors of mass-specific cooling cost ($F_{1,51}$ = 226.4, p < 0.001, r^2 = 0.90), with body mass and thermal conductance accounting for 88.9% and 10% of the variation in cooling cost across species, respectively. Mass-specific cooling cost decreased with increased cooling rate ($F_{1,51}$ = 506.4, p < 0.001, r^2 = 0.91; Fig. 2a), and cooling rate was inversely proportional to body mass ($F_{1,51}$ = 611.1, p < 0.001, r^2 = 0.92; Fig. 2b).

The oft-used 67% proportion of warming cost estimate of cooling cost did not describe cooling cost across taxa (*slope* = 0.07 [-0.03, 0.16], $F_{1,51}$ = 1.83, p = 0.18, r^2 = 0.03; Fig. 3a). Body mass, however, explained 47% of the variation in the difference between the two calculations ($F_{1,51}$ = 44.36, p < 0.001; Fig. 3b). The mean cooling cost was 47.9 ± 18% of warming cost, ranging from 3.8% in *Perognathus longimembris* (8.4 g), the little pocket mouse, to 383% in *T. aculeatus* (4600 g). Cooling cost represented 67% of warming cost in all ground squirrel species and one other species of similar body size: *Callospermophilus lateralis* (137 g, 58% [48–68%]), *Cricetus cricetus* (370 g, 76% [66–86%]), *Ictidomys mexicanus* (190 g, 74% [64–84%]), *I. tridecemlineatus* (190 g, 70% [60–80%]), *Otospermophilus beecheyi* (502 g, 57% [47–67%]), *Spermophilus citellus* (290 g, 58% [48–68%]), *U. parryii* (406 g, 60% [50–70%]), and *U. richardsonii* (406 g, 67% [57–77%]).

4. Discussion

The common assumption that the cost of cooling is equal to 67% of the cost of warming during arousal in hibernation is not broadly applicable across taxa. The cost of cooling scaled with body mass, which was expected given the relationship between the rate of heat loss and surface area to volume ratio (Bakken, 1976a). Consequently, cooling rate was inversely related to mass-specific cooling cost (Fig. 2a), suggesting cooling rate, as a function of body size and thermal conductance, is an important factor in hibernation energetics.

We attributed the mismatch between the two estimates of cooling cost to the fact that the 67% proportion relied on metabolic measurements from a squirrel species (*U. richardsonii*), which has a body mass that is not representative of the body size of most hibernating mammals. Due to the scaling relationship between body mass and surface area (Schmidt-Nielsen, 1984), smaller species have a greater amount of surface exposed to the environment per unit volume compared to larger species (Kleiber, 1972; Strunk, 1971). Greater surface area leads to greater heat loss and thus faster cooling rates, which we observed in the relationship between cooling rate and body mass (Fig. 2b). Therefore, the estimated 67% of the cost of warming overestimated the cost of cooling in species smaller than ground squirrels and underestimated the cost of cooling in larger species (Fig. 3). The fact that most of the variation in the relationship between both cooling cost calculations was described by body mass also supports these patterns. Incorporating both body size and surface area (scaled from body mass) in the calculation of cooling cost leads to more accurate estimates of the differences in cooling across taxa.

In addition to body size differences, body shape can affect cooling cost. Behavioral changes such as posture adjustments may be as important to heat exchange as the physiological properties of an animal (Satinoff, 1978; Stelzner and Hausfater, 1986). Even small postural changes can reduce exposed surface area and alter the amount of heat lost to the environment (Adair, 1976; Sale, 1970). For instance, when exposed to cold environments, captive pigs decrease heat loss by posture adjustments that reduce surface area by as much as 35% (Mount, 1964; Turnpenny et al., 2000). Similarly, *U. richardsonii* curl into a sphere when hibernating (Wang, 1978), whereas other species, such as bats, often remain cylindrical (Gouma et al., 2012). Our model does not consider differences in postural changes, but as the sphere has the least amount of surface area per unit of volume of all geometric shapes (Schmidt-Nielsen, 1970), species of the same body mass may have considerable differences in heat loss due to changes in posture. However, as body size and thermal conductance account for almost 99% of the variation in cooling cost, postural changes could account for only 1% of the variation.

Air temperature can greatly influence the energetic costs associated with both the cooling and warming phases of hibernation: colder environments facilitate a faster rate of cooling and thus lower cooling cost (Bakken, 1976b; Henshaw, 1968) but substantially increase the cost of warming. Therefore, it is no surprise that deriving cooling cost from estimates of warming cost would not be accurate in most species across environments, as T_a has opposite effects on each phase. Though the proportion holds true for *U. richardsonii* in the environments that were measured in the Wang (1978) study, it may misrepresent cooling cost in other environments. By including the effect of T_a in both the cooling and warming models, we include a mechanistic influence of the environment on animal physiology.

The physiological mechanisms behind the cooling and warming processes also suggest it is inappropriate to estimate cooling cost from warming estimates. Warming is considered to be an active process in our analysis, where animals increase T_b using endogenous heat production to warm tissues (Geiser, 2004; but see discussion of passive rewarming below). In placental mammals, brown adipose tissue provides high metabolic heat production for nonshivering thermogenesis (Smalley and Dryer, 1963; Smith and Hock, 1963), while non-placentals (monotremes and marsupials) and birds generate heat by shivering (Johnston, 1971; Schmidt-Nielsen, 1987). Nonshivering thermogenesis has been reported to produce as much heat as shivering in species that do both (Janský, 2008), but the energetic costs of brown fat consumption compared to muscular activity required by shivering have yet to be compared. Differences in the efficiency between these two processes may potentially lead to interspecific differences in warming costs, which makes assumptions inaccurate for some species.

In contrast with active warming, our model assumed that entry into torpor was a passive process – that is, cooling was driven by heat loss rather than active metabolic suppression (Snapp and Heller, 1981). Snapp and Heller (1981) observed that the rate of metabolism decreases in response to temperature, i.e. the Q_{10} effect, supports the hypothesis that most mammals passively enter torpor. However, active metabolic inhibition (e.g. suppression of enzyme activity) may be required for deep torpor (Geiser, 2016, 2004). If active suppression is required for the cooling phase to occur, then cooling rate would also be driven by the ability to inhibit metabolism rather than just body size and thermal conductance. Due to the uncertainty behind when and in which species metabolic inhibition occurs, we assumed passive cooling, and did not account for any changes to metabolic rate. However, our model can be revised to include alterations to input parameters (e.g. metabolic rate) if active suppression alters metabolic rate for a species of interest.

Behavioral mechanisms, such as social thermoregulation, are not considered in our model and may limit model applicability. Social thermoregulation can occur when individuals cluster in hibernation. Social thermoregulation can potentially lead to passive rewarming, which occurs when individuals use increasing T_b of neighbors to synchronize their warming and decrease costs of arousal (Geiser, 2004). Passive rewarming can influence our calculations of warming costs in two different ways. First, lower efficiency of passive rewarming (Arnold, 1988) results in reduced warming rates. Second, because passive rewarming does not have the same energetic requirements of active rewarming, the total energetic cost of warming would be lower in these species (Currie et al., 2015). Although social thermoregulation has been hypothesized to reduce energetic costs associated with arousals and euthermia (Boyles et al., 2008), there has not been an indication of how it may influence cooling. Clustering can increase insulation of individuals and decrease surface area, both of which impede heat loss (Boyles et al., 2008). Though we do not specifically address these issues here, the use of equations to model both cooling and warming allows for modification of functional body size, thermal conductance, or cooling/warming rate once the effect of clustering on these parameters is determined. Using a mathematical equation to predict cooling costs, rather than a general assumption, allows for incorporation of thermoregulatory behavior into energetic modeling.

5. Conclusion

A common assumption used to predict the energetic cost of cooling may not represent cooling cost of all hibernators due to interspecific variation in body size, thermal conductance, and T_a exposure. We considered how mechanisms differed between the cooling and warming processes and how these differences may lead to a mismatch between the assumed proportion and modeled costs. We found that cooling rate scaled linearly with body mass and was a strong predictor of overall cooling cost. Our model allows for generalization of energetic cost for multiple taxa using species-specific physiological and morphometric parameters, and for predictions over variable environmental conditions. Accurate predictions are especially important in the context of wildlife conservation, as the case with predicting the energetic effects of white-nose syndrome on bat species across North America.

Acknowledgements

This project has been funded in part with Federal funds from the Department of Defense Strategic Environmental Research and Development Program [Contract Number W912HQ-16-C-0015]. RP was supported by Defense Advanced Research Projects Agency D16AP00113, National Science Foundation DEB-1716698, National Institutes of Health P20GM103474 and National Institutes of Health P30GM110732. Any opinions, findings, and conclusions or recommendations expressed in this publication are those of the author(s) and do not necessarily reflect the views of the Government.

References

Adair, E.R., 1976. Autonomic thermoregulation in squirrel monkey when behavioral regulation is limited. J. Appl. Physiol. 40, 694–700. https://doi.org/10.1152/jappl.1976.40.5.694.

Armitage, K.B., Blumstein, D.T., Woods, B.C., 2003. Energetics of hibernating yellow-bellied marmots (*Marmota flaviventris*). Comp. Biochem. Physiol. A. Mol. Integr. Physiol. 134, 101–114. https://doi.org/10.1016/S1095-6433(02)00219-2.

Arnold, W., 1988. Social thermoregulation during hibernation in alpine marmots (*Marmota marmota*). J. Comp. Physiol. B 158, 151–156. https://doi.org/10.1007/BF01075828.

Aschoff, J., 1981. Thermal conductance in mammals and birds: its dependence on body size and crcadian phase. Comp. Biochem. Physiol. A Physiol. 69, 611–619. https://doi.org/10.1016/0300-9629(81)90145-6.

Bakken, G.S., 1976a. A heat transfer analysis of animals: unifying concepts and the application of metabolism chamber data to field ecology. J. Theor. Biol. 60, 337–384. https://doi.org/10.1016/0022-5193(76)90063-1.

Bakken, G.S., 1976b. An improved method for determining thermal conductance and equilibrium body temperature with cooling curve experiments. J. Therm. Biol. 1, 169–175. https://doi.org/10.1016/0306-4565(76)90009-7.

Bartholomew, G.A., Cade, T.J., 1957. Temperature regulation, hibernation, and Aestivation in the little pocket mouse, *Perognathus longimembris*. J. Mammal. 38, 60–72. https://doi.org/10.2307/1376476.

Bartholomew, G.A., MacMillen, R.E., 1961. Oxygen consumption, estivation, and hibernation in the kangaroo mouse, *Microdipodops pallidus*. Physiol. Zool. 34, 177–183.

Berman, A., 2003. Effects of body surface area estimates on predicted energy requirements and heat stress. J. Dairy Sci. 86, 3605–3610. https://doi.org/10.3168/jds.S0022-0302(03)73966-6.

Blehert, D.S., Hicks, A.C., Behr, M., Meteyer, C.U., Berlowski-Zier, B.M., Buckles, E.L., Coleman, J.T.H., Darling, S.R., Gargas, A., Niver, R., Okoniewski, J.C., Rudd, R.J., Stone, W.B., 2009. Bat white-nose syndrome: an emerging fungal pathogen? (227–227). Science 323. https://doi.org/10.1126/science.1163874.

Boyer, B.B., Barnes, B.M., 1999. Molecular and metabolic aspects of mammalian hibernation: expression of the hibernation phenotype results from the coordinated regulation of multiple physiological and molecular events during preparation for and entry into torpor. BioScience 49, 713–724. https://doi.org/10.2307/1313595.

Boyles, J.G., Brack, V., 2009. Modeling survival rates of hibernating mammals with individual-based models of energy expenditure. J. Mammal. 90, 9–16. https://doi.org/10.1644/08-MAMM-A-205.1.

Boyles, J.G., McKechnie, A.E., 2010. Energy conservation in hibernating endotherms: why “suboptimal” temperatures are optimal. Ecol. Model. 221, 1644–1647. https://doi.org/10.1016/j.ecolmodel.2010.03.018.

Boyles, J.G., Storm, J.J., Brack, V., 2008. Thermal benefits of clustering during hibernation: a field test of competing hypotheses on *Myotis sodalis*. Funct. Ecol. 22, 632–636.

Boyles, J.G., Willis, C.K., 2010. Could localized warm areas inside cold caves reduce mortality of hibernating bats affected by white-nose syndrome? Front. Ecol. Environ. 8, 92–98. https://doi.org/10.1890/080187.

Burles, D.W., Fenton, M.B., Barclay, R.M., Brigham, R.M., Volkers, D., 2014. Aspects of the winter ecology of bats on Haida Gwaii, British Columbia. Northwest. Nat 95, 289–299. https://doi.org/10.1898/12-32.1.

Cranford, J.A., 1983. Body temperature, heart rate and oxygen consumption of normothermic and heterothermic western jumping mice (*Zapus princeps*). Comp. Biochem. Physiol. A 74, 595–599.

Cryan, P.M., Wolf, B.O., 2003. Sex differences in the thermoregulation and evaporative water loss of a heterothermic bat, *Lasiurus cinereus*, during its spring migration. J. Exp. Biol. 206, 3381–3390. https://doi.org/10.1242/jeb.00574.

Currie, S.E., Noy, K., Geiser, F., 2015. Passive rewarming from torpor in hibernating bats: minimizing metabolic costs and cardiac demands. Am. J. Physiol. Regul. Integr. Comp. Physiol. 308, R34–R41. https://doi.org/10.1152/ajpregu.00341.2014.

Czenze, Z.J., Jonasson, K.A., Willis, C.K.R., 2017. Thrifty females, frisky males: winter energetics of hibernating bats from a cold climate. Physiol. Biochem. Zool. 90, 502–511. https://doi.org/10.1086/692623.

Czenze, Z.J., Willis, C.K.R., 2015. Warming up and shipping out: arousal and emergence timing in hibernating little brown bats (*Myotis lucifugus*). J. Comp. Physiol. [B] 185, 575–586. https://doi.org/10.1007/s00360-015-0900-1.

Drew, K.L., Buck, C.L., Barnes, B.M., Christian, S.L., Rasley, B.T., Harris, M.B., 2007. Central nervous system regulation of mammalian hibernation: implications for metabolic suppression and ischemia tolerance. J. Neurochem. 102, 1713–1726. https://doi.org/10.1111/j.1471-4159.2007.04675.x.

Dunbar, M.B., 2007. Thermal energetics of torpid silver-haired bats *Lasionycteris noctivagans*. Acta Theriol. (Warsz.) 52, 65–68. https://doi.org/10.1007/BF03194200.

Dunbar, M.B., Tomasi, T.E., 2006. Arousal patterns, metabolic rate, and an energy budget of Eastern red bats (*Lasiurus borealis*) in winter. J. Mammal. 87, 1096–1102.

Ehlman, S.M., Cox, J.J., Crowley, P.H., 2013. Evaporative water loss, spatial distributions, and survival in white-nose-syndrome-affected little brown myotis: a model. J. Mammal. 94, 572–583. https://doi.org/10.1644/12-MAMM-A-111.1.

Fleming, M.R., 1985. The thermal physiology of the feathertail glider *Acrobates pygmaeus* (Marsupialia: burramyidae). Aust. J. Zool. 33, 667–681.

Florant, G.L., Heller, H.C., 1977. CNS regulation of body temperature in euthermic and hibernating marmots *(Marmota flaviventris*). Am. J. Physiol. 232, R203–R208. https://doi.org/10.1152/ajpregu.1977.232.5.R203.

Frederico, P., 2007. Bat Population Dynamics: an Individual-based Model Approach (Ph.D. Dissertation). University of Tennessee.

Geiser, F., 2016. Conserving energy during hibernation. J. Exp. Biol. 219, 2086–2087. https://doi.org/10.1242/jeb.129171.

Geiser, F., 2004. Metabolic rate and body temperature reduction during hibernation and daily torpor. Annu. Rev. Physiol. 66, 239–274. https://doi.org/10.1146/annurev.physiol.66.032102.115105.

Geiser, F., 1988. Reduction of metabolism during hibernation and daily torpor in mammals and birds: temperature effect or physiological inhibition? J. Comp. Physiol. B 158, 25–37. https://doi.org/10.1007/BF00692726.

Geiser, F., 1987. Hibernation and daily torpor in two pygmy possums (*Cercartetus* Spp., Marsupialia). Physiol. Zool. 60, 93–102.

Geiser, F., Baudinette, R.V., 1990. The relationship between body mass and rate of rewarming from hibernation and daily torpor in mammals. J. Exp. Biol. 151, 349–359.

Geiser, F., Baudinette, R.V., 1988. Daily torpor and thermoregulation in the small Dasyurid marsupials *Planigale gilesi* and *Ningaui yvonneae*. Aust. J. Zool. 36, 473–481.

Geiser, F., Baudinette, R.V., 1987. Seasonality of torpor and thermoregulation in three dasyurid marsupials. J. Comp. Physiol. B 157, 335–344. https://doi.org/10.1007/BF00693360.

Geiser, F., Brigham, R.M., 2000. Torpor, thermal biology, and energetics in Australian long-eared bats (*Nyctophilus*). J. Comp. Physiol. B 170, 153–162. https://doi.org/10.1007/s003600050270.

Geiser, F., Kenagy, G.J., 1988. Torpor duration in relation to temperature and metabolism in hibernating ground squirrels. Physiol. Zool. 61, 442–449.

Glantz, S., Slinker, B., 2000. Primer of Applied Regression & Analysis of Variance, 2 ed. McGraw-Hill Education / Medical, New York.

Gouma, E., Simos, Y., Verginadis, I., Lykoudis, E., Evangelou, A., Karkabounas, S., 2012. A simple procedure for estimation of total body surface area and determination of a new value of Meeh's constant in rats. Lab. Anim. 46, 40–45. https://doi.org/10.1258/la.2011.011021.

Grigg, G.C., Augee, M.L., Beard, L.A., 1992. Thermal Relations of Free-living Echidnas During Activity and in Hibernation in a Cold Climate. pp. 160–173.

Halsall, A.L., Boyles, J.G., Whitaker, J.O., 2012. Body temperature patterns of big brown bats during winter in a building hibernaculum. J. Mammal. 93, 497–503. https://doi.org/10.1644/11-MAMM-A-262.1.

Hart, J.S., 1951. Calorimetric determination of average body temperature of small mammals and its variation with environmental conditions. Can. J. Zool. 29, 224–233. https://doi.org/10.1139/z51-021.

Hayman, D.T.S., Pulliam, J.R.C., Marshall, J.C., Cryan, P.M., Webb, C.T., 2016. Environment, host, and fungal traits predict continental-scale white-nose syndrome in bats. Sci. Adv. 2, e1500831. https://doi.org/10.1126/sciadv.1500831.

Heldmaier, G., Ortmann, S., Elvert, R., 2004. Natural hypometabolism during hibernation and daily torpor in mammals. Respir. Physiol. Neurobiol. 141, 317–329. https://doi.org/10.1016/j.resp.2004.03.014.

Heldmaier, G., Ruf, T., 1992. Body temperature and metabolic rate during natural hypothermia in endotherms. J. Comp. Physiol. B 162, 696–706. https://doi.org/10.1007/BF00301619.

Henshaw, R.E., 1968. Thermoregulation during hibernation: application of Newton's law of cooling. J. Theor. Biol. 20, 79–90. https://doi.org/10.1016/0022-5193(68)90093-3.

Herreid, C.F., Kessel, B., 1967. Thermal conductance in birds and mammals. Comp. Biochem. Physiol. 21, 405–414. https://doi.org/10.1016/0010-406X(67)90802-X.

Herreid, C.F., Schmidt-Nielsen, K., 1966. Oxygen consumption, temperature, and water loss in bats from different environments. Am. J. Physiol. 211, 1108–1112.

Hirshfeld, J.R., O'Farrell, M.J., 1976. Comparisons of differential warming rates and tissue temperatures in some species of desert bats. Comp. Biochem. Physiol. A 55, 83–87.

Hock, R.J., 1960. Seasonal variations in physiologic functions of arctic ground squirrels and black bears. Bull. Mus. Comp. Zool. 124, 155–171.

Hope, P.R., Jones, G., 2012. Warming up for dinner: torpor and arousal in hibernating Natterer's bats (*Myotis nattereri*) studied by radio telemetry. J. Comp. Physiol. B 182, 569–578. https://doi.org/10.1007/s00360-011-0631-x.

Hosken, D.J., Withers, P.C., 1997. Temperature regulation and metabolism of an Australian bat, *Chalinolobus gouldii* (Chiroptera: vespertilionidae) when euthermic and torpid. J. Comp. Physiol. [B] 167 71–80.

Hudson, J.W., 1965. Temperature regulation and torpidity in the pygmy mouse, *Baiomys taylori*. Physiol. Zool. 38, 243–254.

Humphries, M.M., Thomas, D.W., Speakman, J.R., 2002. Climate-mediated energetic constraints on the distribution of hibernating mammals. Nature 418, 313–316. https://doi.org/10.1038/nature00828.

Hut, R.A., Barnes, B.M., Daan, S., 2002. Body temperature patterns before, during, and after semi-natural hibernation in the European ground squirrel. J. Comp. Physiol. [B] 172, 47–58.

Janský, L., 2008. Non-shivering thermogenesis and its thermoregulatory significance. Biol. Rev. 48, 85–132. https://doi.org/10.1111/j.1469-185X.1973.tb01115.x.

Johansen, K., Krog, J., 1959. Diurnal body temperature variations and hibernation in the birchmouse, *Sicista betulina*. Am. J. Physiol. -Leg. Content 196, 1200–1204. https://doi.org/10.1152/ajplegacy.1959.196.6.1200.

Johnston, D.W., 1971. The absence of brown adipose tissue in birds. Comp. Biochem. Physiol. A Physiol. 40, 1107–1108. https://doi.org/10.1016/0300-9629(71)90298-2.

Jonasson, K.A., Willis, C.K.R., 2012. Hibernation energetics of free-ranging little brown bats. J. Exp. Biol. 215, 2141–2149. https://doi.org/10.1242/jeb.066514.

Kayser, C., 1964. La depense d'energie des mammiferes en hibernation. Arch. Sci. Physiol. (Paris) 18, 137–150.

Kayser, C., 1961. The Physiology of Natural Hibernation. Pergamon Press.

Kenagy, G.J., Vleck, D., 1982. Daily temporal organization of metabolism in small mammals: adaptation and diversity. In: Vertebrate Circadian Systems, Proceedings in Life Sciences. Springer, Berlin, Heidelberg, pp. 322–338. https://doi.org/10.1007/978-3-642-68651-1_35.

Kleiber, M., 1972. Body size, conductance for animal heat flow and Newton's law of cooling. J. Theor. Biol. 37, 139–150. https://doi.org/10.1016/0022-5193(72)90120-8.

Langwig, K.E., Frick, W.F., Bried, J.T., Hicks, A.C., Kunz, T.H., Marm Kilpatrick, A., 2012. Sociality, density-dependence and microclimates determine the persistence of populations suffering from a novel fungal disease, white-nose syndrome. Ecol. Lett. 15, 1050–1057. https://doi.org/10.1111/j.1461-0248.2012.01829.x.

Langwig, K.E., Frick, W.F., Hoyt, J.R., Parise, K.L., Drees, K.P., Kunz, T.H., Foster, J.T., Kilpatrick, A.M., 2016. Drivers of variation in species impacts for a multi-host fungal disease of bats. Philos. Trans. R. Soc. B 371, 20150456. https://doi.org/10.1098/rstb.2015.0456.

Larkin, J.E., Heller, H.C., 1996. Temperature sensitivity of sleep homeostasis during hibernation in the golden-mantled ground squirrel. Am. J. Physiol. 270, R777–R784. https://doi.org/10.1152/ajpregu.1996.270.4.R777.

Lee, T.N., Kohl, F., Buck, C.L., Barnes, B.M., 2016. Hibernation strategies and patterns in sympatric arctic species, the Alaska marmot and the arctic ground squirrel. J. Mammal. 97, 135–144. https://doi.org/10.1093/jmammal/gyv163.

Licht, P., Leitner, P., 1967. Physiological responses to high environmental temperatures in three species of microchiropteran bats. Comp. Biochem. Physiol. 22, 371–387. https://doi.org/10.1016/0010-406X(67)90601-9.

Lorch, J.M., Muller, L.K., Russell, R.E., O'Connor, M., Lindner, D.L., Blehert, D.S., 2013. Distribution and environmental persistence of the causative agent of white-nose syndrome, *Geomyces destructans*, in bat hibernacula of the eastern United States. Appl. Environ. Microbiol. 79, 1293–1301. https://doi.org/10.1128/AEM.02939-12.

Lyman, C.P., 2013. Hibernation and Torpor in Mammals and Birds. Elsevier.

Lyman, C.P., 1948. The oxygen consumption and temperature regulation of hibernating hamsters. J. Exp. Zool. 109, 55–78. https://doi.org/10.1002/jez.1401090105.

Marom, S., Korine, C., Wojciechowski, M.S., Tracy, C.R., Pinshow, B., 2006. Energy metabolism and evaporative water loss in the European free-tailed bat and Hemprich's long-eared bat (Microchiroptea): species sympatric in the Negev Desert. Physiol. Biochem. Zool. PBZ 79, 944–956. https://doi.org/10.1086/505999.

Mayberry, H.W., McGuire, L.P., Willis, C.K.R., 2018. Body temperatures of hibernating little brown bats reveal pronounced behavioural activity during deep torpor and suggest a fever response during white-nose syndrome. J. Comp. Physiol. [B] 188, 333–343. https://doi.org/10.1007/s00360-017-1119-0.

McGuire, L.P., Jonasson, K.A., Guglielmo, C.G., 2014. Bats on a budget: torpor-assisted migration saves time and energy. PLoS One 9, e115724. https://doi.org/10.1371/journal.pone.0115724.

McGuire, L.P., Mayberry, H.W., Willis, C.K.R., 2017. White-nose syndrome increases torpid metabolic rate and evaporative water loss in hibernating bats. Am. J. Physiol. Regul. Integr. Comp. Physiol. 313, R680–R686. https://doi.org/10.1152/ajpregu.00058.2017.

McKechnie, A.E., Wolf, B.O., 2004. The energetics of the rewarming phase of avian torpor. In: Barnes, B.M., Carey, H.V. (Eds.), Life in the Cold: Evolution, Mechanisms, Adaptiation, and Applications. International Hibernation Symposium Institute of Arctic Biology, University of Alaska, Fairbanks, Alaska.

Meeh, K., 1879. Oberflächenmessungen des menschlichen Körpers. Z. Biol. 15, 425–458.

Menzies, A.K., Webber, Q.M.R., Baloun, D.E., McGuire, L.P., Muise, K.A., Coté, D., Tinkler, S., Willis, C.K.R., 2016. Metabolic rate, latitude and thermal stability of roosts, but not phylogeny, affect rewarming rates of bats. Physiol. Behav. 164, 361–368. https://doi.org/10.1016/j.physbeh.2016.06.015.

Mount, L.E., 1964. Radiant and convective heat loss from the new-born pig. J. Physiol. 173, 96–113.

Nagel, A., 1977. Torpor in the European white-toothed shrews. Experientia 33, 1455–1456. https://doi.org/10.1007/BF01918804.

Neal, C.M., 1976. Energy budget of the eastern chipmunk (*Tamias* striatus): convective heat loss. Comp. Biochem. Physiol. A 54, 157–160.

Neumann, R.L., Cade, T.J., 1965. Torpidity in the Mexican ground squirrel *Citellus mexicanus parvidens* (mearns). Can. J. Zool. 43, 133–140. https://doi.org/10.1139/z65-011.

Newton, I., 1701. Scala graduum caloris, Calorum descriptiones & signa (scale of the degrees of heat). Philos. Trans. 22, 74–829.

Nicol, S.C., Andersen, N.A., 2007. Cooling rates and body temperature regulation of hibernating echidnas (*Tachyglossus aculeatus*). J. Exp. Biol. 210, 586–592. https://doi.org/10.1242/jeb.02701.

O'Farrell, M.J., Studier, E.H., 1970. Fall metabolism in relation to ambient temperatures in three species of Myotis. Comp. Biochem. 35–697.

Ortmann, S., Heldmaier, G., 2000. Regulation of body temperature and energy requirements of hibernating alpine marmots (*Marmota marmota*). Am. J. Physiol. Regul. Integr. Comp. Physiol. 278, R698–R704.

Pajunen, I., 1970. Body temperature, heart rate, breathing pattern, weight loss and periodicity of hibernation in the Finnish garden dormouse, *Eliomys quercinus* L. Ann. Zool. Fenn. 7, 251–266.

Pohl, H., Hart, J.S., 1965. Thermoregulation and cold acclimation in a hibernator, *Citellus tridecemlincatus*. J. Appl. Physiol. 20, 398–404. https://doi.org/10.1152/jappl.1965.20.3.398.

Pretzlaff, I., Dausmann, K.H., 2012. Impact of climatic variation on the hibernation physiology of *Muscardinus avellanarius*. In: Living in a Seasonal World. Springer, Berlin, Heidelberg, pp. 85–97. https://doi.org/10.1007/978-3-642-28678-0_8.

Prothero, J., Jürgens, K.D., 1986. An energetic model of daily torpor in endotherms. J. Theor. Biol. 121, 403–415. https://doi.org/10.1016/S0022-5193(86)80099-6.

R Development Core Team, 2009. R: a Language and Environment for Statistical Computing. R Foundation for Statistical Computing, Vienna, Austria.

Reeder, D.M., Frank, C.L., Turner, G.G., Meteyer, C.U., Kurta, A., Britzke, E.R., Vodzak, M.E., Darling, S.R., Stihler, C.W., Hicks, A.C., Jacob, R., Grieneisen, L.E., Brownlee, S.A., Muller, L.K., Blehert, D.S., 2012. Frequent arousal from hibernation linked to severity of infection and mortality in bats with white-nose syndrome. PLoS One 7, e38920. https://doi.org/10.1371/journal.pone.0038920.

Sale, J.B., 1970. The behaviour of the resting rock hyrax in relation to its environment. Zool. Afr. 5, 87–99. https://doi.org/10.1080/00445096.1970.11447383.

Satinoff, E., 1978. Neural organization and evolution of thermal regulation in mammals. Science 201, 16–22.

Schmidt-Nielsen, K., 1987. Animal Physiology: Adaptation and Environment, 3rd ed. Cambridge University Press, London ; New York.

Schmidt-Nielsen, K., 1984. Scaling: Why is Animal Size so Important?, 1 ed. Cambridge University Press, Cambridge ; New York.

Schmidt-Nielsen, K., 1970. Energy metabolism, body size, and problems of scaling. Fed. Proc. 29, 1524–1532.

Smalley, R.L., Dryer, R.L., 1963. Brown fat: thermogenic effect during arousal from hibernation in the bat. Science 140, 1333–1334.

Smith, R.E., Hock, R.J., 1963. Brown fat: thermogenic effector of arousal in hibernators. Science 140, 199–200.

Snapp, B.D., Heller, H.C., 1981. Suppression of metabolism during hibernation in ground squirrels (*Citellus lateralis*). Physiol. Zool. 54, 297–307. https://doi.org/10.1086/physzool.54.3.30159944.

Snyder, G.K., Nestler, J.R., 1990. Relationships between body temperature, thermal conductance, Q10 and energy metabolism during daily torpor and hibernation in rodents. J. Comp. Physiol. B 159, 667–675. https://doi.org/10.1007/BF00691712.

Song, X., Körtner, G., Geiser, F., 1997. Thermal relations of metabolic rate reduction in a hibernating marsupial. Am. J. Physiol. 273, R2097–R2104.

Song, X., Körtner, G., Geiser, F., 1995. Reduction of metabolic rate and thermoregulation during daily torpor. J. Comp. Physiol. B 165, 291–297. https://doi.org/10.1007/BF00367312.

Speakman, J.R., Thomas, D.W., 2003. Physiological ecology and energetics of bats. In: Kunz, T.H., Fenton, M.B. (Eds.), Bat Ecology. University Of Chicago Press, Chicago and London, pp. 430–490.

Staples, J.F., 2014. Metabolic suppression in mammalian hibernation: the role of mitochondria. J. Exp. Biol. 217, 2032–2036. https://doi.org/10.1242/jeb.092973.

Stelzner, J.K., Hausfater, G., 1986. Posture, microclimate, and thermoregulation in yellow baboons. Primates 27, 449–463. https://doi.org/10.1007/BF02381890.

Stone, G.N., Purvis, A., 1992. Warm-up rates during arousal from torpor in heterothermic mammals: physiological correlates and a comparison with heterothermic insects. J. Comp. Physiol. B 162, 284–295.

Strumwasser, F., 1959. Thermoregulatory, brain and behavioral mechanisms during entrance into hibernation in the squirrel, *Citellus beecheyi*. Am. J. Physiol. 196, 15–22.

Strunk, T.H., 1971. Heat loss from a Newtonian animal. J. Theor. Biol. 33, 35–61. https://doi.org/10.1016/0022-5193(71)90215-3.

Thomas, D.W., Dorais, M., Bergeron, J.-M., 1990. Winter energy budgets and cost of arousals for hibernating little brown bats, *Myotis lucifugus*. J. Mammal. 71, 475–479. https://doi.org/10.2307/1381967.

Tucker, V.A., 1965. Oxygen consumption, thermal conductance, and torpor in the California pocket mouse *Perognathus californicus*. J. Cell. Comp. Physiol. 65, 393–403. https://doi.org/10.1002/jcp.1030650313.

Turnpenny, J.R., Wathes, C.M., Clark, J.A., McArthur, A.J., 2000. Thermal balance of livestock: 2. applications of a parsimonious model. Agric. For. Meteorol. 101, 29–52. https://doi.org/10.1016/S0168-1923(99)00157-4.

Wang, L., Hudson, J.W., 1970. Some physiological aspects of temperature regulation in the normothermic and torpid hispid pocket mouse, *Perognathus hispidus*. Comp. Biochem. Physiol. 32, 275–293. https://doi.org/10.1016/0010-406X(70)90941-2.

Wang, L.C.H., 1978. Energetics and field aspects of mammalian torpor: the Richardson's ground squirrel. In: Wang, L.C.H., Hudson, J.W. (Eds.), Strategies in the Cold. Academic Press, New York, pp. 109–145.

Warnecke, L., Turner, J.M., Bollinger, T.K., Lorch, J.M., Misra, V., Cryan, P.M., Wibbelt, G., Blehert, D.S., Willis, C.K.R., 2012. Inoculation of bats with European *Geomyces destructans* supports the novel pathogen hypothesis for the origin of white-nose syndrome. Proc. Natl. Acad. Sci. USA 109, 6999–7003. https://doi.org/10.1073/pnas.1200374109.

Warnecke, L., Turner, J.M., Bollinger, T.K., Misra, V., Cryan, P.M., Blehert, D.S., Wibbelt, G., Willis, C.K.R., 2013. Pathophysiology of white-nose syndrome in bats: a mechanistic model linking wing damage to mortality. Biol. Lett. 9, 20130177. https://doi.org/10.1098/rsbl.2013.0177.

Waßmer, T., Wollnik, F., 1997. Timing of torpor bouts during hibernation in European hamsters (*Cricetus cricetus L.*). J. Comp. Physiol. B 167, 270–279. https://doi.org/10.1007/s003600050074.

Webb, P.I., Ellison, J., 1998. Normothermy, torpor, and arousal in hedgehogs (*Erinaceus europaeus*) from Dunedin. N. Z. J. Zool. 25, 85–90. https://doi.org/10.1080/03014223.1998.9518139.

Wilcox, A., Willis, C.K., 2016. Energetic benefits of enhanced summer roosting habitat for little brown bats (*Myotis lucifugus*) recovering from white-nose syndrome. Conserv. Physiol. 4, cov070.

Willis, C.K., 2015. Conservation physiology and conservation pathogens: white-nose syndrome and integrative biology for host–pathogen systems. Integr. Comp. Biol. 55, 631–641.

Willis, C.K.R., 2008. Do roost type or sociality predict warming rate? A phylogenetic analysis of torpor arousal. In: Lovegrove, B.G., McKechnie, A.E. (Eds.), Hypometabolism in Animals: Hibernation, Torpor and Cryobiology. School of Biological and Conservation Sciences, University of KwaZulu-Natal, Pietermaritzburg, pp. 373–384.

Willis, C.K.R., Brigham, R.M., Geiser, F., 2006. Deep, prolonged torpor by pregnant, free-ranging bats. Naturwissenschaften 93, 80–83. https://doi.org/10.1007/s00114-005-0063-0.

Willis, C.K.R., Menzies, A.K., Boyles, J.G., Wojciechowski, M.S., 2011. Evaporative water loss is a plausible explanation for mortality of bats from white-nose syndrome. Integr. Comp. Biol. 51, 364–373. https://doi.org/10.1093/icb/icr076.

Wilz, M., Heldmaier, G., 2000. Comparison of hibernation, estivation and daily torpor in the edible dormouse, *Glis glis*. J. Comp. Physiol. B 170, 511–521. https://doi.org/10.1007/s003600000129.

Wojciechowski, M.S., Jefimow, M., Tegowska, E., 2007. Environmental conditions, rather than season, determine torpor use and temperature selection in large mouse-eared bats (*Myotis myotis*). Comp. Biochem. Physiol. A. Mol. Integr. Physiol. 147, 828–840. https://doi.org/10.1016/j.cbpa.2006.06.039.